

The Reaction of Cubic Sodium Tungsten Bronzes, Na_xWO_3 , with Metallic Iron

I. J. MCCOLM AND S. J. WILSON*

School of Industrial Technology, University of Bradford, Bradford 7, England

Received March 2, 1979; in final form August 13, 1979

The reaction of the cubic sodium bronzes, Na_xWO_3 , with powdered iron metal has been studied by heating samples *in vacuo* and also at high pressure. Evidence for reaction is found at unexpectedly low temperatures. The reaction is an overall reduction which proceeds via an increase in the sodium content of the bronze phase up to some temperature-dependent limiting composition for which $x < 1$. The existence of this limit, its temperature dependence, and the identity of the other products of reduction have been explained in terms of the partial oxygen pressure of the system. The course of the reduction has been followed through the evolution of the bronze lattice parameter and a reaction mechanism is postulated. No evidence of significant incorporation of iron into a stable cubic sodium bronze phase has been found.

Introduction

The sodium tungsten bronzes have frequently been assumed to be chemically inert, although, apart from a study of the reduction of sodium bronzes by hydrogen (1), very few accounts of their chemical properties have been published. In acid media the sodium bronzes do appear to be inert although in the presence of alkalis they may be oxidized by species such as $\text{Ag}(1)$ and fericyanide (2) and even slowly by oxygen. The property of inertness to nonoxidizing acids allied to that of electrical conductivity has led to the possibility of their use as electrodes in fuel cells. Consequently a number of electrochemical studies of the catalysis of hydrogen oxidation and oxygen reduction reactions by sodium bronzes in acid media have appeared (3-6). The activity of sodium bronzes as catalysts for a number of gas

reactions has also been investigated; for example, the catalytic decomposition of formic acid (7). Hence it is surprising that no data are available on the reactivity of sodium bronzes at elevated temperatures with potential container materials. The aim of this report is to describe the reaction between cubic sodium bronzes, Na_xWO_3 , and iron metal.

The properties of tungsten bronzes have been shown to depend more on the number of valence electrons donated to the WO_3 lattice than on the identity of the inserted cation itself (8-11). Thus the fact that iron tungsten bronzes have such a low limiting iron content (12, 13) may, it was felt, be of importance in determining the reaction pathways in this system.

Experimental Details

Samples of well-sintered sodium tungsten bronzes were prepared by the solid state reaction $(x/2)\text{Na}_2\text{WO}_4 + ((3 - 2x)/3)\text{WO}_3 + (x/6)\text{W} = \text{Na}_x\text{WO}_3$. Anhydrous Na_2WO_4

* Present address: Department of Mineralogy and Petrology, Downing Place, University of Cambridge, England.

was prepared by heating $\text{Na}_2\text{WO}_4 \cdot 2\text{H}_2\text{O}$ (Analar B.D.H.) at 120°C for 12 hr. The reactants were heated in an evacuated silica tube at 850°C for times ranging from 3 to 7 days and then cooled slowly to room temperature. The reactions between the sodium bronzes and powdered iron metal were also performed *in vacuo*, in sealed silica tubes. For high-pressure synthesis the sample was encapsulated in Pt foil and heated at pressure within a phrophyllite test cell using a tetrahedral anvil apparatus. A Stanton Redcroft instrument was used for the DTA experiments with both samples and reference material enclosed in evacuated silica ampoules.

Samples were routinely examined by X-ray powder techniques, using a Philips 114.6-mm-diameter Debye-Scherrer camera and an IRDAB 100-mm-diameter Guinier focusing camera with CuK_α radiation.

Accurate lattice parameters for cubic bronze phases were obtained by Nelson-Riley extrapolation of high-angle Debye-Scherrer reflections (estimated accuracy $\pm 0.0003 \text{ \AA}$). The compositions of the cubic Na_xWO_3 phases were calculated from the Brown-Banks equation (14):

$$a_0 = 0.0819x + 3.7846 \text{ \AA},$$

relating lattice parameter to composition (estimated accuracy in x , ± 0.004).

A variety of optical microscopes were used to visually compare the morphology of each product phase.

Results

Samples of cubic sodium tungsten bronzes with metallic Fe fired *in vacuo* at 1100°C produced a fused mass which X-ray and optical examination showed to consist of a cubic bronze with imprecise lattice parameters because of the breadth and lack of definition of the X-ray lines together with FeWO_4 and WO_2 embedded in a flux of

sodium tungstate species. Firing at 950°C , while not resulting in complete fusion, also produced samples containing an ill-defined cubic bronze with sodium tungstate and polytungstates.

DTA examination of similar bronze/Fe mixes showed the main feature to be a large endothermic peak in heating cycles at about 1000°C . Subsequent heating cycles revealed the presence of small sharp endotherms in the region $575\text{--}700^\circ\text{C}$ which increase in size on successive cycles and are characteristic of Na_2WO_4 and $\text{Na}_2\text{W}_2\text{O}_7$. X-Ray examination showed that the products of DTA cycling are similar to the $950\text{--}1100^\circ\text{C}$ furnace-fired samples with the cubic bronze phase giving a diffuse powder pattern. A DTA experiment involving cycling up to 865°C produced a sample containing a well-defined cubic bronze phase with only FeWO_4 and WO_2 , indicating that reaction with the iron took place. That the large 1000°C endotherm is not related to the reaction with Fe was confirmed by a DTA experiment on a pure sodium tungsten bronze which also gave a large endotherm at about 1000°C and was subsequently found to contain tungstate phases. The overall picture obtained then is one of a reaction between the cubic sodium bronze and metallic Fe occurring at low to moderate temperatures followed by decomposition of the bronze phase starting at about 900°C and producing sodium tungstates. Accordingly, investigation of the bronze/Fe reaction was conducted by preparing *in vacuo* furnace-fired samples at temperatures below 900°C .

Data for such samples are presented in Table I, in which the compositions of bronze product phases have been calculated from the Brown-Banks equation (14) assuming them to be pure sodium bronzes. The presence of small amounts of unreacted Fe was detected magnetically. The physical form of the bronze product phases, polyhedral at lower temperatures, becomes distinctly globular for the 850°C samples which

TABLE I
 $\text{Na}_x\text{WO}_3 + y\text{Fe}$ SAMPLES

Sample	Treatment (°C)	Bronze color	X-ray phase analysis ^a	Cube lattice parameters, Å, and compositions, (x)	
$\text{Na}_{0.479}\text{WO}_3 + 0.053 \text{ Fe}$ 86	650 40 hr	Blue/purple	S Cube	3.8238	
		Dark red	ms Smaller cube	3.8343(0.607)	
			mw FeWO_4 mw WO_2	3.8259	
$\text{Na}_{0.479}\text{WO}_3 + 0.055 \text{ Fe}$	355 66 hr	Blue/purple	s Cube	3.8238	
		Dark purple	vw Smaller cube + Fe	3.8243(0.485)	
	63	450 70 hr	Purple	s Cube	3.8242(0.484)
				vw Smaller cube + Fe	
	52	650 41 hr	Dark red	s Cube	3.8326(0.586)
				m Smaller cube w FeWO_4 w WO_2	3.8239
	70	650 1128 hr	Mauve/red	s Cube	3.8299(0.553)
				mw FeWO_4 mw WO_2	
	59	750 70 hr	Red/mauve	s Cube	3.8294(0.547)
				mw FeWO_4 mw WO_2	
24	850 66 hr	Purple	s Cube	3.8284(0.535)	
			w FeWO_4 w WO_2		
$\text{Na}_{0.479}\text{WO}_3 + 0.092 \text{ Fe}$	64	Blue/purple	s Cube + Fe	3.8238	
		Blue/purple		3.8241(0.482)	
	78	590 48 hr	Dark red	s Cube	3.8325(0.585)
				vw Smaller cube	~3.825
				mw FeWO_4 mw $\text{WO}_2 + \text{Fe}$	
	53	650 29 hr	Red	s Cube	3.8396(0.672)
				m Smaller cube m FeWO_4 mw WO_4	3.8247
54	800 113 hr	Dark red	s Cube	3.8334(0.596)	
			vw Smaller cube m FeWO_4 m WO_2	~3.821	
$\text{Na}_{0.479}\text{WO}_3 + 0.173 \text{ Fe}$ 84	850 42 hr	Blue/purple	s Cube	3.8238	
		Red	in FeWO_4	3.8364(0.632)	
			mw W vw WO_2		
$\text{Na}_{0.479}\text{WO}_3 + 0.207 \text{ Fe}$ 79	590 48 hr	Blue/purple	s Cube	3.8238	
		Red/orange	vw Smaller cube	3.8376(0.647)	
			m FeWO_4	~3.827	
			mw WO_2		
			w W + Fe		

TABLE I—Continued

Sample	Treatment (°C)	Bronze color	X-ray phase analysis ^a	Cube lattice parameters, Å, and compositions, (x)
67	650 98 hr	Orange/brown	s Cube mw FeWO ₄ mw WO ₂ + Fe	3.8433(0.717)
74	850 164 hr	Orange/red	s Cube w FeWO ₄ mw W	3.8402(0.679)
Na _{0.547} WO ₃ + 0.63 Fe		Red/mauve		3.8294
90	650 20 hr	Dark red	s Cube w FeWO ₄ vw WO ₂	3.8317(0.575)
91	650 48 hr	Dark red	s Cube mw FeWO ₄ mw WO ₂	3.8328(0.589)
92	650 165 hr	Dark red	s Cube mw FeWO ₄ w WO ₂	3.8326(0.586)
93	650 600 hr	Dark red	s Cube mw FeWO ₄ w WO ₂	3.8321(0.580)
Na _{0.547} WO ₃ + 0.100 Fe		Red/mauve		3.8294
50	750 65 kb 2 hr	Red	s Cube mw FeWO ₄ vw WO ₂ w Hexagonal bronze	3.8395(0.670)
Na _{0.589} WO ₃ + 0.049 Fe		Dark red		3.8328
66	650 98 hr	Brick red	s Cube mw FeWO ₄ mw WO ₂	3.8398(0.674)
26	850 115 hr	Red/orange	s Cube mw FeWO ₄ w WO ₂ vw W	3.8383(0.656)
Na _{0.646} WO ₃ + 0.061 Fe		Orange		3.8375
65	650 65 hr	Orange/brown	s Cube w FeWO ₄ w WO ₂ vw W + Fe	3.8367(0.636)
21	850 91 hr	Orange	s Cube mw FeWO ₄ mw W	3.8417(0.697)
Na _{0.656} WO ₃ + 0.049 Fe		Orange		3.8383
80	590 48 hr	Orange	s Cube m W	3.8388(0.662)
51	650 24 hr	Orange/brown	s Cube w FeWO ₄ mw W vw WO ₂ + Fe	3.8402(0.679)

TABLE I—Continued

Sample	Treatment (°C)	Bronze color	X-ray phase analysis ^a	Cube lattice parameters, Å, and compositions, (x)
22	850 98 hr	Red/orange	s Cube w FeWO_4 mw W	3.8414(0.694)
$\text{Na}_{0.741}\text{WO}_3 + 0.050 \text{ Fe}$ 75	850 164 hr	Orange/brown Red/orange	s Cube mw FeWO_4 w W mw Na_2WO_4	3.8453 3.8407(0.685)
$\text{Na}_{0.773}\text{WO}_3 + 0.053 \text{ Fe}$ 77	850 115 hr	Orange/brown Orange	s Cube m WFeWO_4 m W m Na_2WO_4	3.8479 3.8426(0.708)
$\text{Na}_{0.853}\text{WO}_3 + 0.106 \text{ Fe}$ 68	650 98 hr	Yellow Yellow ochre	s Cube w FeWO_4 vw W+Fe	3.8545 3.8552(0.862)
73	850 164 hr	Orange	s Cube m FeWO_4 mw W m Na_2WO_4	3.8430(0.713)

^a s = strong; m = medium; mw = medium weak; w = weak; vw = very weak.

have the appearance of a mass of metallic droplets, perhaps indicating that the temperature at which the bronze itself starts to decompose is being approached.

The most important general result to be derived from Table I is that the reaction between the sodium bronzes and Fe metal seems to start at a remarkably low temperature. This is in contrast to the assumed chemical inertness of the bronzes. At 450°C, changes in bronze color and cubic unit-cell parameter provide evidence of reaction. Even at 355°C there are indications of slight reaction.

Decomposition products first become detectable in X-ray patterns of samples fired at 590°C. FeWO_4 is always among these but the identity of the others seems to depend on the original bronze composition. The WO_2 found for the lower bronzes is replaced by W

as x increases. For the highest bronzes, Na_2WO_4 also appears as a decomposition product. The bronze product phases, except for those from the highest original bronze compositions, have colors and lattice parameters characteristic of an increase in the value of x and, in all cases, these show a variation with the firing temperature. Although the visual evidence of color can only be a rough guide, the changes in color and cubic unit-cell parameter appear to be parallel and there are no obvious discrepancies between observed color and composition calculated on the basis of a pure sodium bronze phase. Thus there is no obvious evidence of wholesale insertion of Fe cations into the sodium bronze structure. The final feature of the data is that the nature of the variation of a_0 with temperature depends on the original bronze composition.

The most striking example of this is the coexistence of two distinct cubic phases, each with a sharp powder pattern and most marked at about 650°C, for the reactions of the lowest sodium bronze.

The plots of Fig. 1 show clearly the nature of the variation of cubic unit-parameter with firing temperature. For the reactions with 0.05 mole Fe the Na_{0.479}WO₃ bronze exhibits a clear maximum and the coexistence of two cubic phases; the Na_{0.589}WO₃ bronze shows a smaller maximum and the higher bronzes none at all. For the reactions of Na_{0.479}WO₃ with varying amounts of Fe (Fig. 1b), the presence of two cubic bronze phases is again observed and the degree of separation of the two cubic cell parameters

increases with the amount of Fe in the reaction mixture.

The question arises as to whether these plots represent a near-equilibrium situation at each temperature or whether they can be viewed as following the path of the reaction in a mechanistic sense. Certainly the presence of excess metallic Fe even in some of the 650°C fired samples indicates that complete reaction has not been accomplished at this stage, while the 850°C fired samples have bronze product cell parameters approaching those expected on the basis of complete reaction according to one of the two reaction schemes:

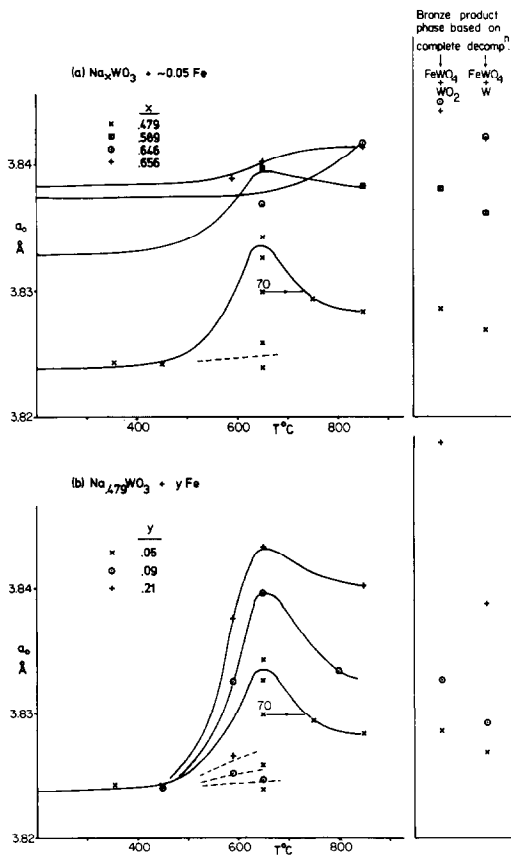
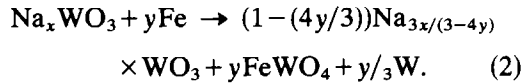
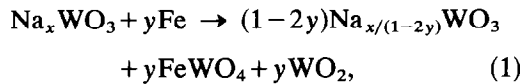


FIG. 1. Variation of bronze parameter with firing temperature for bronze + Fe reactions.

Figure 1 shows that with an increase in x or y there is a tendency for scheme (1) to be replaced by scheme (2).

If the plots of Fig. 1 do in fact follow the path of the reaction, then the bronze product cell parameters should show a similar dependence on firing time. Figure 2 shows some a_0 against time plots for two lower bronze + Fe reactions at 650°C. Although the accuracy in measured a_0 is probably no better than ± 3 in the fourth place the observed maximum is probably real.

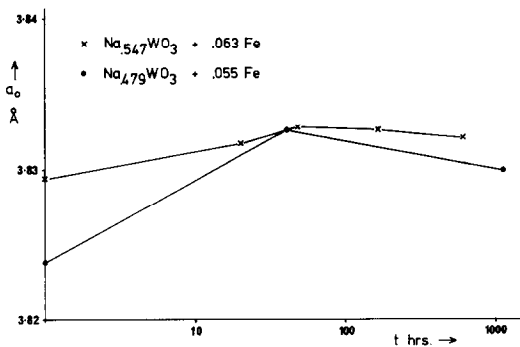


FIG. 2. Variation of bronze parameter with firing time at 650°C.

For a solid state reaction which will be essentially controlled kinetically by processes involving diffusion it seems reasonable that the course of the reaction may be conveniently frozen at various intermediate stages by using similar firing times at a variety of temperatures. Certainly a comparison of samples 52 and 70 reveals that an increase of nearly 30-fold in firing time at 650°C produces a product similar to that expected after a short firing at 725°C . Thus, since firing times of other samples varied to a much smaller extent, in discussing the possible reaction mechanism the plots of Fig. 1 will be regarded as representing a reasonable approximation of the reaction path.

Since the 850°C fired samples seem to represent a situation close to completion of the bronze + Fe reaction, phase relationships for such samples are presented in Fig. 3. Here the tie lines have been drawn solely on the basis of the cubic cell lattice parameters,

assuming the bronze phase to be a pure sodium bronze. When extrapolated to the Fe_y axis these tie lines give good agreement with the observed reaction products so that little error is introduced by making such an assumption.

The compositions prepared indicate three important regions in Fig. 3. For low values of x and y the reaction follows scheme (1), producing a higher sodium bronze together with FeWO_4 and WO_2 .

An increase in x or y results in the pivoting of the tie lines about some point on the Na_x axis so that scheme (2) is followed with W metal rather than WO_2 becoming the stable reaction product. Certainly the results of Table I reveal that in general either W or WO_2 is produced rather than mixtures of the two. The most notable feature of Fig. 3 is that there appears to be a maximum composition for the bronze product phase of $x \approx 0.71$. For reactions $\text{Na}_x\text{WO}_3 + y\text{Fe}$ at 850°C with high

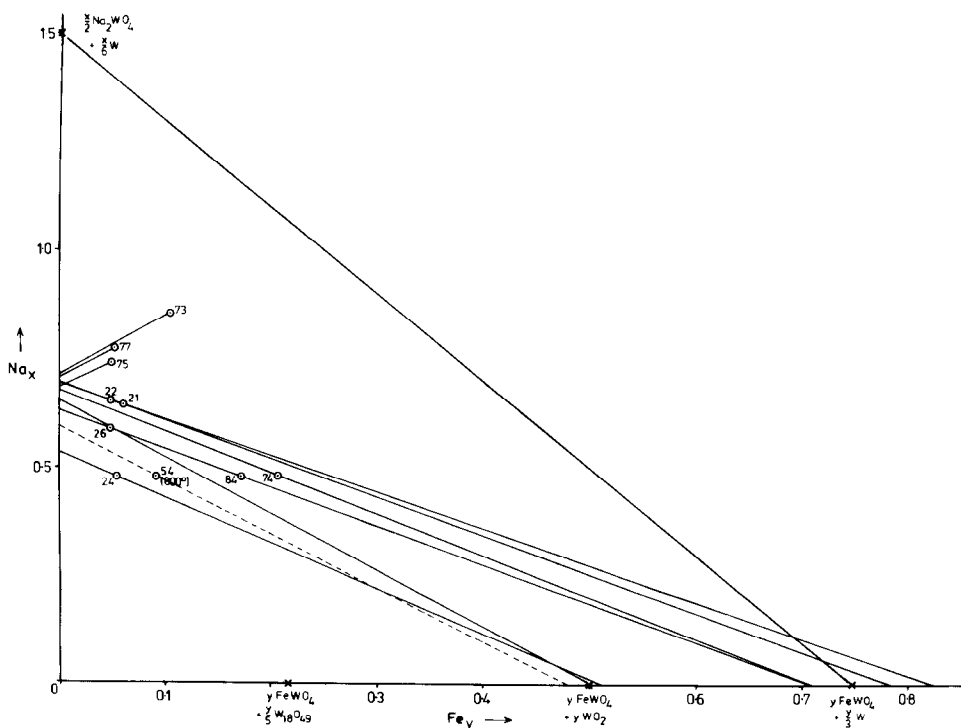


FIG. 3. Phase relationships for $\text{Na}_x\text{WO}_3 + y\text{Fe}$ samples fired at 850°C .

values of x a third reaction scheme is followed such that this limiting bronze product, $\text{Na}_{\sim 0.7}\text{WO}_3$, is formed together with Na_2WO_4 , FeWO_4 , and W .

In order to compare these results with those at other temperatures and since the reaction of cubic sodium bronzes with Fe could not conveniently be brought to completion at temperatures lower than 850°C , a number of samples in the $\text{Na}_x\text{Fe}_y\text{WO}_3$ system were prepared from mixtures of tungstates Na_2WO_4 and FeWO_4 with WO_3 and W at temperatures below 850°C . These samples verified the results from the 850°C Fe plus bronze work. For example, $\text{Na}_{0.6}\text{Fe}_{0.21}\text{WO}_3$ prepared at 850°C contained Na_2WO_4 and a sodium bronze with $x = 0.73$. This can be compared to the limiting value of $x = 0.71$ found for bronze plus Fe samples at the same temperature. The same overall composition heated only to 650°C led to a sodium bronze with $x = 0.88$ and no evidence for Na_2WO_4 . Thus the upper limiting composition in the presence of iron is apparently very temperature dependent.

Discussion

The overall reaction between cubic sodium tungsten bronzes and metallic Fe *in vacuo* can be considered as a reduction of the bronze. The Fe is oxidized to FeWO_4 while the bronze reduction products depend on the stoichiometry, $\text{Na}_x\text{WO}_3 + y\text{Fe}$. For low values of x or y , reaction scheme (1) is followed, producing a higher bronze, FeWO_4 and WO_2 . For slightly higher values of x or y reaction scheme (2) is followed and W metal replaces WO_2 as a reduction product. There appears to be an upper limit to the composition of the bronze product phase (X) and for values of x and y such that $3x/3 - 4y > X$ the reaction products are the limiting bronze, Na_xWO_3 , together with Na_2WO_4 , FeWO_4 , and W . In the presence of sufficient Fe ($y = 3 - 2x/4$) one should

expect complete reduction to Na_2WO_4 , FeWO_4 , and W .

The formation of a bronze product phase with increased Na content (up to some limit, X) can be regarded as an intermediate stage in the overall reduction process. It is a feature of the reduction of the widely nonstoichiometric Na_xWO_3 bronzes that, in the presence of insufficient Fe for complete reduction, partial reduction does not produce Na_2WO_4 , FeWO_4 , and W together with unchanged excess reactant, but that the range of possible values of x allows for intermediate degrees of reduction to be achieved. Such features must be accounted for in discussing possible reaction mechanisms.

In the case of reduction by hydrogen (1) the composition of sodium bronzes increased up to the limit $x = 1$ imposed by the perovskite structure. For reduction by metallic Fe the limiting composition has $x < 1$ and, furthermore, is dependent on the temperature of reaction. At 850°C values for the limiting composition of $x \approx 0.71$ (bronze + Fe reactions) and 0.73 (tungstate mixes) were found, while at 650°C the limit is somewhat greater than 0.88 . This phenomenon must be a function of the presence of Fe in the system.

Mechanism

Any mechanism proposed for the reaction must account for the form of the a_0 vs T curves of Fig. 1. In the case of an interface reaction one would expect a gradual increase in the bronze unit-cell parameter to that of the ultimate product as the reaction proceeds. For the lower bronzes this behavior was not observed. The a_0 vs T curves exhibit a maximum and, for the lower bronze (0.479), two cubic bronze phases were found to coexist during the early stages of reduction. The smaller of these two cubic unit cells does not represent unreacted starting material even though it has a similar lattice

parameter. The larger cubic phase always has the stronger X-ray powder intensity, while the smaller phase appears first, with very low intensity, at $\approx 450^\circ\text{C}$ and reaches its highest intensity in 650°C fired samples, when the parameter separation is at its largest, before disappearing.

A possible reaction mechanism which explains the shape of the a_0 vs T curves, the coexistence of two cubic bronze phases, and the observed variation in their X-ray intensities can be developed. Such a mechanism does not involve decomposition at the bronze/Fe interface but requires initial diffusion of Fe into the bronze lattice. The production of an Fe-rich surface layer in the bronze crystallites represents a nonequilibrium situation in terms both of the Fe concentration gradient set up and of the increased electron concentration associated with the Fe-rich zone. The obvious way for this to be resolved is for the Fe to become evenly distributed throughout the lattice.

However, to explain the observed formation of two distinct cubic phases a lower mobility must be postulated for Fe than for Na in the bronze lattice. The nonequilibrium situation is then resolved by the diffusion of Na cations away from the Fe-rich zone producing two cubic bronze regions, one a mixed Na-Fe bronze and the other a pure Na bronze with increased Na content, with an overall constant electron concentration. Because of the smaller size of Fe as an insertion cation, the mixed bronze has always the smaller parameter and this explains the observed intensity behavior. The more mobile Na cations partition themselves between the two regions so as to maintain this constant electron concentration in both. Thus as more Fe diffuses in, the sodium content of the larger cubic unit cell increases to a maximum. Previous work on tungsten bronzes has often indicated that the number and valence of inserted elements are more important in determining properties than their identity. This proposed mechanism

makes use of this fact, and by suggesting an unequal distribution of inserted cations in a bronze lattice with a constant electron concentration, perhaps indicates the necessity of talking in terms of "electron bronzes" rather than sodium or iron bronzes.

If this idea of a constant electron concentration is valid it is possible to imagine a situation in which both Fe and Na concentration gradients are set up within the crystallites. However, the X-ray patterns reveal two sharp, distinct cubic unit-cell phases. This may be explained by assuming a lower mobility for Fe and a very low upper limit to the concentration of Fe allowed in the bronze lattice. Certainly in the Fe_xWO_3 system the maximum possible value of X is about 0.03 (12, 15).

The next step in the mechanism is the decomposition of the Fe-rich region, perhaps on reaching some critical composition, to give FeWO_4 and WO_2 or W. This leaves behind a depleted sodium bronze phase with a lattice continuous with that of the Na-rich region so that redistribution of the Na cations must then occur, producing a decrease in overall Na content and hence a decrease in the cubic lattice parameter toward that of the ultimate decomposition product.

The differing behavior of the higher sodium bronzes perhaps indicates increased difficulty of Fe diffusion due to the smaller number of vacancies. Reduction thus takes place at the interface with the mobility of Na cations in the bronze lattice allowing a gradual change of cell parameter toward that of the final product.

The feasibility of the partial reduction of a sodium bronze by Fe to a higher bronze, FeWO_4 and WO_2 or W, is shown by the good agreement between the results obtained and those predicted by reaction schemes (1) and (2).

The proposed model requires a lower mobility for Fe than for Na in the bronze lattice. An experiment was designed in which two pure sodium bronzes, with a separation

in lattice parameter similar to that found in samples containing two bronze phases, were reacted together under conditions which produced the double cubic phase behavior in bronze+Fe reactions. $\text{Na}_{0.547}\text{WO}_3$ and $\text{Na}_{0.646}\text{WO}_3$ (overall composition $\text{Na}_{0.610}\text{WO}_3$) were reacted at 650°C for 42 hr and produced a single cubic bronze phase with $a_0 = 3.8341 \text{ \AA}$ ($x = 0.604$). Thus, two pure Na_xWO_3 phases cannot coexist under these conditions, so that the double cube reduction intermediate must incorporate Fe in some way.

In order to study the distribution of products in a compacted reaction mixture, a bronze+Fe sample was heated under a high pressure (sample 50; Table I), producing a dense, red, metallic cylinder. The composition of the cubic bronze phase in this sample

agrees well with that predicted by reaction scheme (1). The presence of a small amount of a hexagonal bronze phase was unexpected since this structure is generally only found for tungsten bronzes containing large inserted cations. However, it does appear that this structure is favored at high pressures, since under these conditions it has also been found for bronzes containing a number of smaller cations such as Li (16), Na (17), Ba, Ca, and Sr (18), and Fe (13).

A polished section of this high-pressure sample showed a microstructure of which Fig 4 is typical. Microprobe analysis allowed identification of the three phases which can be distinguished. First there is the red bronze matrix which is fine grained but shows some larger crystal faces. Second, a gold metallic material, FeWO_4 , appears as nodules with a

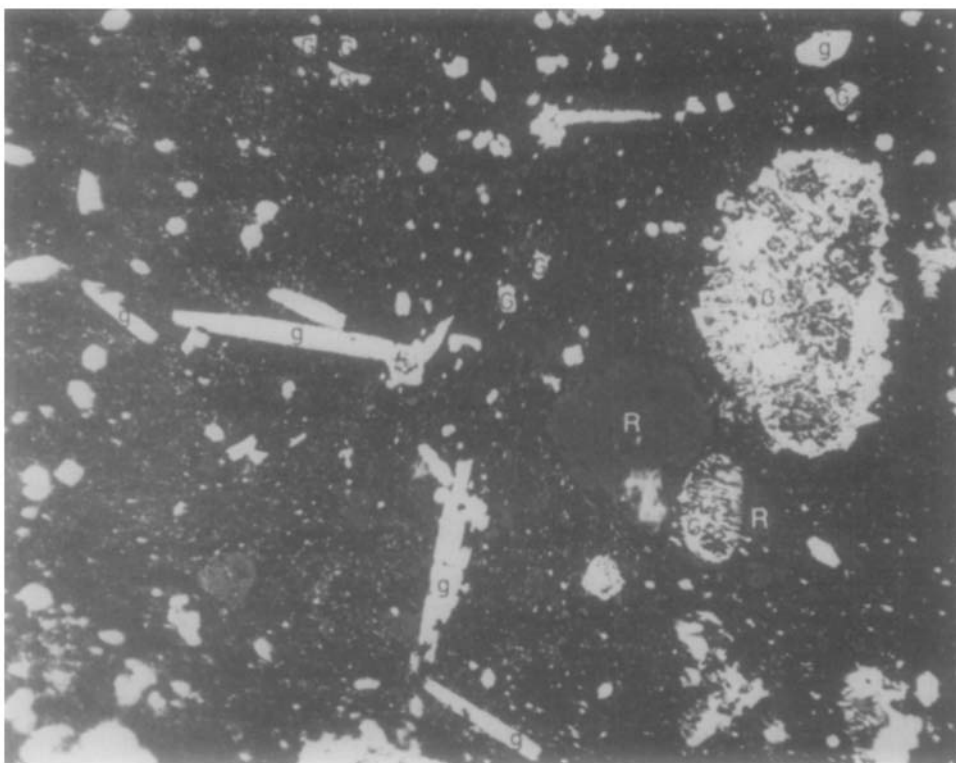


FIG. 4. Microstructure of high-pressure sample from $\text{Na}_{0.547}\text{WO}_3 + 0.1 \text{ Fe}$. Magnification, $\times 300$. g = gray, G = gold, R = red matrix.

radiating structure, some of which contain residual iron metal at their centers, and as smaller angular fragments. Third, a gray material was found to be WO₂, occurring as acicular and angular crystal fragments. The red bronze matrix gave a background count for Fe, some of which is undoubtedly due to scattered white radiation, indicative of an Fe concentration of less than 0.03 wt%. This is equivalent to a value of y in Na_{0.67}Fe _{y} WO₃ of less than 0.001.

The microstructure of Fig. 4 reveals that, apart from the accumulation of the gold material in nodules and around the small amount of residual Fe, both gold and gray phases appear as small fragments distributed randomly throughout the bronze matrix. In the case of reaction at the bronze/Fe interface one would expect close association of FeWO₄ and WO₂ in the product. Thus, although the course of the bronze + Fe reaction may be different at high pressures, the results of this experiment do not disagree with the proposed mechanism involving diffusion of Fe followed by decomposition. In addition it provides evidence of an insignificant Fe content in the bronze product phase.

Thermodynamic Analysis of the Reaction

The results of the bronze + Fe reactions show that reduction of the bronze proceeds via an increase in Na content up to a limiting composition Na _{x} WO₃ where $x < 1$, in contrast to the reduction by H₂ where a limit of $x = 1$ is observed. In considering the stability range of the sodium bronzes rather than the process of reduction, the implication is that in the presence of Fe the limit to the value of x in Na _{x} WO₃ is lower than the structural limit ($x = 1$) imposed by the perovskite structure and observed in the pure Na _{x} WO₃ system. Furthermore the value of this limit is temperature dependent. An explanation for these phenomena should perhaps be sought by consideration of the

role of the partial oxygen pressure in the system.

The Fe-W-O system has been investigated by Schmahl and Dillenberg (19) by equilibration with CO/CO₂ mixtures at 900°C. Their results on the stability ranges of the various phases were expressed as the percentage of CO₂ in the equilibrium gas mixture, and from these the P_{O_2} data of Table II have been calculated. Apart from the equilibria involving Fe₂WO₆ and Fe these data apply also to the binary W-O system. It should be noted though that the phase labeled WO_{2.75} by Schmahl and Dillenberg is unknown and probably refers to the phase W₁₈O₄₉ (WO_{2.72}). As far as the Fe-W-O system is concerned the important result is that, at 900°C, FeWO₄ is stable only in the range of $P_{O_2} = 2.924 \times 10^{-18}$ to 4.997×10^{-12} atm. In order to see what bearing these results might have on the stability of sodium bronzes in the presence of Fe, it is necessary to obtain P_{O_2} data for the Na _{x} WO₃ system at 900°C.

Whittingham and Dickens (1) have measured the oxygen partial pressure above sodium bronzes in equilibrium with their oxidation products at 750°C by the use of a zirconia solid state electrolyte, and also by measuring open circuit potentials during electrolytic preparation of the bronzes.

Thus, for the reaction:

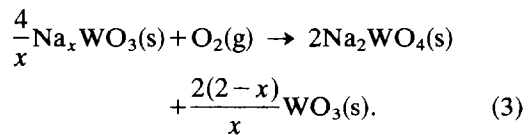


TABLE II
Fe-W-O SYSTEM: P_{O_2} DATA, 900°C

Phases in equilibrium	P_{O_2} (atm)	log P_{O_2}
Fe ₂ WO ₆ -FeWO ₄ -WO ₃	4.997×10^{-12}	-11.30
FeWO ₄ -WO ₃ -WO _{2.75}	3.949×10^{-15}	-14.30
FeWO ₄ -WO _{2.75} -WO ₂	5.266×10^{-17}	-16.28
FeWO ₄ -WO ₂ -W	8.487×10^{-18}	-17.07
Fe-FeWO ₄ -W	2.924×10^{-18}	-17.53

The available thermodynamic data consist of the partial oxygen pressure, the easily derived equilibrium constant, at 750°C, and a value of $\Delta H^\circ_{298} = -440$ kJ/mole (20). In order to calculate equivalent P_{O_2} data at other temperatures specific heat data for the phases in reaction (3) were obtained. For oxygen, an empirical power series (21) for the range 790–1500°K was used:

$$C_p = 21.4861 + 2.6350 \times 10^{-2} T - 1.7197 \times 10^{-5} T^2 + 4.2568 \times 10^{-9} T^3 \text{ J/(mole}\cdot^\circ\text{K)},$$

while for the solid phases Kopp's rule was assumed. This is an application of Dulong and Petit's rule to ionic solids and states that the molar heat capacity of a solid compound is the sum of the atomic heats of its component elements (26.8 J/(g·atom·°K) for most elements). Available specific heat data for WO_3 at 1000°K (22), Na_2WO_4 at 300°K (21), and Na_xWO_3 at 800°K (23) indicate that this behavior is indeed approached at high temperatures. Thus for reaction (3)

$$\begin{aligned} \Delta C_p &= (2 \times 26.8) - 21.4861 - 2.6350 \times 10^{-2} T \\ &\quad + 1.7197 \times 10^{-5} T^2 \\ &\quad - 4.2568 \times 10^{-9} T^3 \text{ J/(mole}\cdot^\circ\text{K)} \\ &= \left(\frac{\partial \Delta H}{\partial T} \right)_p, \text{ by Kirchoff's equation.} \end{aligned}$$

Integration, and use of the value of ΔH°_{298} , gives:

$$\begin{aligned} \Delta H_T^\circ &= -448543 + 32.1139 T - 1.3175 \times 10^{-2} T^2 \\ &\quad + 5.7323 \times 10^{-6} T^3 - 1.0642 \times 10^{-9} T^4 \text{ J/mole.} \end{aligned}$$

Using van't Hoff's isochore, integration of the function $\Delta H/T^2$ gives:

$$\begin{aligned} R \ln \frac{Kp_2}{Kp_1} &= \left[\frac{448543}{T} + 32.1139 \ln T \right. \\ &\quad - 1.3175 \times 10^{-2} T + 2.8662 \times 10^{-6} T^2 \\ &\quad \left. - 3.5473 \times 10^{-10} T^3 \right]_{T_1}^{T_2} \text{ J/(mole}\cdot^\circ\text{K)}. \quad (4) \end{aligned}$$

Use of this equation allowed calculation of Kp , and thus P_{O_2} , for the bronze oxidation reaction at a number of temperatures from Whittingham and Dickens' 750°C data (Table III). The bronze P_{O_2} data calculated for 900°C are plotted in Fig. 5, together with the data on phase stability regions for the Fe–W–O system.

One aspect of the experimental results can now be explained. Since the $FeWO_4:WO_2:W:O_2$ system is univariant there will only be one partial oxygen pressure

TABLE III

THEMODYNAMIC DATA FOR THE REACTION: $(4/x)Na_x(WO_3(s) + O_2(g)) \rightarrow 2Na_2WO_4(s) + (2(2-x)/x)WO_3(s)$

x in Na_xWO_3	750°C ^a		900°C		850°C		650°C	
	$\ln Kp_{1023}$	$\log P_{O_2}$	$\ln Kp_{1173}$	$\log P_{O_2}$	$\ln Kp_{1123}$	$\log P_{O_2}$	$\ln Kp_{923}$	$\log P_{O_2}$
0.2	24.64	-10.7	18.28	-7.94	20.21	-8.77	30.06	-13.05
0.3	27.40	-11.9	21.04	-9.14	22.97	-9.97	32.82	-14.25
0.4	30.85	-13.4	24.49	-10.63	26.42	-11.47	36.27	-15.75
0.5	35.00	-15.2	28.64	-12.44	30.57	-13.27	40.42	-17.55
0.6	39.38	-17.1	33.02	-14.34	34.95	-14.18	44.8	-19.46
0.7	44.67	-19.4	38.31	-16.64	40.24	-17.47	50.09	-21.75
0.8	51.12	-22.2	44.76	-19.44	46.69	-20.28	56.54	-24.55

^a 750°C data derived from Whittingham and Dickens (1).

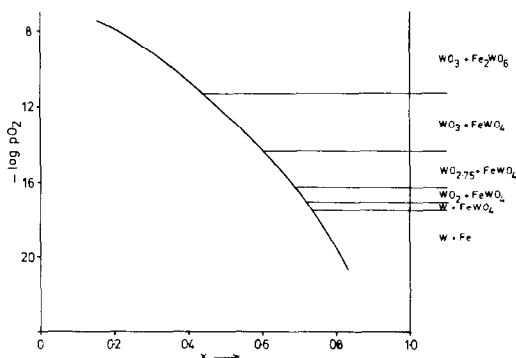


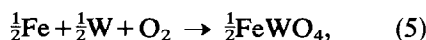
FIG. 5. P_{O_2} calculated for Na_xWO_3 , and phase stability ranges calculated for the Fe-W-O system at 900°C .

(at a particular temperature) at which all four will be in equilibrium. Hence the general observation that WO_2 and W do not appear together as decomposition products.

A more important feature of these thermodynamic considerations is that the presence of FeWO_4 imposes a lower limit to the P_{O_2} of the system. In the case of hydrogen reduction of a bronze the maximum composition of the bronze product is limited only by the stoichiometry of the perovskite structure since the P_{O_2} for $\text{H}_2 + \text{H}_2\text{O}$ at $900^\circ\text{C} = 10^{-30}$ atm. In the presence of FeWO_4 the minimum P_{O_2} (2.92×10^{-18} atm at 900°C) imposes a maximum on the composition of stable bronze phases. From Fig. 5 this would appear to be at $x \approx 0.735$ for 900°C and this compares well with the experimental 850°C values of $x = 0.71-0.73$, despite the broad assumptions made during the derivation.

In order to explain the observed variation in limiting bronze composition with temperature, the value of the lower limit of P_{O_2} in the presence of FeWO_4 was determined for a number of other temperatures.

Using the value of P_{O_2} at 900°C shown in Table II gives $Kp_{1173} = 3.420 \times 10^{17}$ for the reaction:



and $\Delta G^\circ_{1173} = -393.75$ kJ/mole.

To calculate ΔG° at other temperatures, use was made of the equation:

$$\left(\frac{\partial \Delta G}{\partial T}\right)_p = -\Delta S.$$

Ignoring entropies of the solid phases, $-\Delta S$ was taken as equal to S_{O_2} which is itself temperature dependent according to:

$$\left(\frac{\partial S}{\partial T}\right)_p = \frac{C_p}{T}.$$

Using a general power series for the heat capacity of O_2 (24),

$$C_p = 25.723 + 1.30 \times 10^{-2}T - 3.85 \times 10^{-6}T^2 \text{ J/(mole}\cdot^\circ\text{K)}.$$

Integration of C_p/T and taking S_{298} for $\text{O}_2 = 205.03$ J(mole $\cdot^\circ\text{K}$) (22) gives:

$$\begin{aligned} S &= 54.781 + 25.723 \ln T + 1.30 \times 10^{-2}T \\ &\quad - 1.93 \times 10^{-6}T^2 \text{ J(mole}\cdot^\circ\text{K)} \\ &= -\Delta S \text{ for reaction (5)}. \end{aligned}$$

Further integration and use of the value of ΔG°_{1173} gives:

$$\begin{aligned} \Delta G^\circ_T &= -648984 + 29.058T \\ &\quad + 25.723T \ln T + 6.50 \times 10^{-3}T^2 \\ &\quad - 6.43 \times 10^{-7}T^3 \text{ J/mole}. \end{aligned} \quad (6)$$

Use of this equation allows calculation of ΔG° , and thus Kp and P_{O_2} , for reaction (5) with the results shown in Table IV. The value

TABLE IV
THERMODYNAMIC DATA FOR THE REACTION $\frac{1}{2}\text{Fe} + \frac{1}{2}\text{W} + \text{O}_2 \rightarrow \frac{1}{2}\text{FeWO}_4$ AND ESTIMATED LIMITING BRONZE COMPOSITIONS Na_xWO_3 , IN THE PRESENCE OF FeWO_4

Temp. ($^\circ\text{K}$)	ΔG°_T (kJ/mole)	$\ln Kp$	$\log P_{\text{O}_2}$	Limiting bronze composition (x)
923	-455.0	59.3	-25.75	0.83
1023	-430.8	50.6	-22.00	0.795
1123	-406.2	43.5	-18.89	0.755
1173	-393.75	40.4	-17.53	0.735

of $\log P_{O_2}$ listed is thus the lowest at which $FeWO_4$ can exist in the Na_xWO_3-Fe system. By plotting these limiting P_{O_2} values with the corresponding bronze P_{O_2} vs x curves as in Fig. 6, the estimates of the maximum stable bronze composition at each temperature in the presence of $FeWO_4$ (shown in Table IV) were obtained. It will be noted that they display the same trend toward a decrease in limiting bronze composition with increasing temperature that was observed for the samples prepared in the $Na_xFe_yWO_3$ system.

Conclusions

The cubic sodium bronzes, Na_xWO_3 , react with Fe metal at quite low temperatures, the reaction commencing at about $400^\circ C$. The overall reaction can be described as a reduction of the bronze to Na_2WO_4 and W and proceeds via an increase in the Na content of the bronze phase up to some temperature-dependent limiting composition for which $x < 1$. This implies that in the presence of Fe the composition range for stable Na_xWO_3 phases is decreased. The existence of an upper limit to bronze composition and its variation with temperature, together with

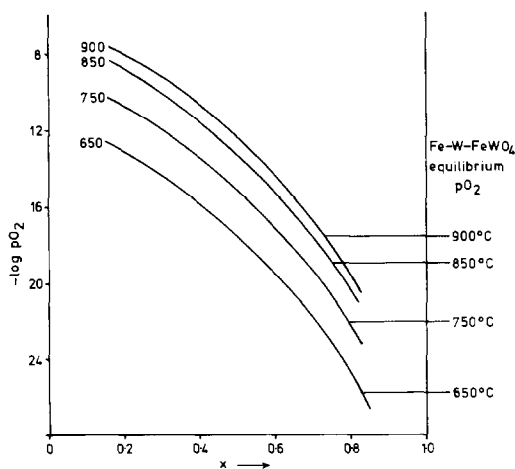


FIG. 6. Partial oxygen pressures for sodium bronzes and for the equilibrium: $\frac{1}{2}Fe + \frac{1}{2}W + O_2 \rightarrow \frac{1}{2}FeWO_4$, plotted at a number of temperatures.

the identity of the other reaction products, are determined by the partial oxygen pressure imposed on the system by the presence of $FeWO_4$.

The course of partial reduction to a higher bronze phase has been followed by means of the evolution of the bronze lattice parameter, and was found to vary with the original bronze composition. For the low sodium content cubic bronzes a mechanism is proposed involving initial diffusion of Fe into the bronze lattice up to some low limiting composition, partition of the more highly mobile Na^+ cations to maintain a constant electron concentration, and final decomposition. For higher bronzes a mechanism involving reduction at the bronze/Fe interface appears to be more appropriate.

No evidence for significant insertion of Fe cations into the cubic sodium bronze lattice has been found, except for the formation of the reaction intermediate during the reduction of the lower bronzes.

Acknowledgments

S.J.W. was in receipt of an S.R.C. studentship during the time of this work. We wish to thank Mr. J. Penfold of the S.T.L. high-pressure laboratory for assisting with the high-pressure work and S.R.C. for providing the finance. Mr. Whitaker also of S.T.L. did the microprobe examination of which we make grateful acknowledgment.

References

1. M. S. WHITTINGHAM AND P. G. DICKENS, in "Proceedings, 7th International Symposium on the Reactivity of Solids," p. 640, Bristol (1972).
2. P. G. DICKENS AND D. J. NEILD, *J. Chem. Soc. Dalton*, 1074 (1973).
3. B. BROYDE, *J. Catal.* **10**, 13 (1968).
4. R. D. ARMSTRONG, A. F. DOUGLAS, AND D. E. WILLIAMS, *Energy Convers.* **11**, 7 (1971).
5. J. P. RANDIN, *J. Electrochem. Soc.* **121**, 1029 (1974).
6. J. VONDRAK AND J. BALEJ, *Collect. Czech. Chem. Commun.* **40**, 3298 (1975).
7. S. S. MOODY AND D. TAYLOR, *J. Chem. Soc. Faraday Trans. 1* **69**, 289 (1973).

8. J. M. REAU, C. FOUASSIER, G. LEFLEM, J. Y. BARRAUD, J. P. DOUMERC, AND P. HAGENMULLER, *Rev. Chim. Miner.* **7**, 975 (1970).
9. W. OSTERTAG, *Inorg. Chem.* **5**, 758 (1966).
10. E. BIALKOWSKA, E. POLACZKOWA, A. POLACZEK, AND A. GESICKI, *Bull. Acad. Pol. Sci. Ser. Sci. Chim.* **21**, 137 (1973).
11. I. J. MCCOLM AND S. J. WILSON, *J. Solid State Chem.* **26**, 223 (1978).
12. I. J. MCCOLM, R. J. D. TILLEY, C. P. M. BARTON, AND N. N. GREENWOOD, *J. Solid State Chem.* **16**, 265 (1976).
13. I. J. MCCOLM, R. STEADMAN, AND S. J. WILSON, *J. Solid State Chem.* **23**, 33 (1978).
14. B. W. BROWN AND E. BANKS, *J. Amer. Chem. Soc.* **76**, 963 (1954).
15. J. P. DOUMERC, G. SCHIFFMACHER, P. CARO, AND M. POUCHARD, *C.R. Acad. Sci. Paris Ser. C* **282**, 295 (1976).
16. T. E. GIER, D. C. PEASE, A. W. SLEIGHT, AND T. A. BITHER, *Inorg. Chem.* **7**, 1646 (1968).
17. T. A. BITHER, J. L. GILLSON, AND H. S. YOUNG, *Inorg. Chem.* **5**, 1559 (1966).
18. P. E. BIERSTEDT, T. A. BITHER, AND F. J. DARNELL, *Solid State Commun.* **4**, 25 (1966).
19. N. G. SCHMAHL AND H. DILLENBURG, *Z. Phys. Chem. Neue Folge* **77**, 113 (1972).
20. P. G. DICKENS AND P. J. WISEMAN, in "MTP International Review of Science," Ser. 2: "Inorganic Chemistry" (L. E. J. Roberts, Ed.), Vol. 10, Chap. 7, Butterworths, London (1975).
21. Y. S. TOULOUKIAN AND C. Y. HO (Eds), "Thermophysical Properties of Matter," TPRC Data Series, IFI/Plenum, New York (1970).
22. D. R. STULL *et al.*, "JANAF Thermochemical Tables," Nat. Bur. Stand., Washington, D.C. (1965).
23. H. INABA AND K. NAITO, *J. Solid State Chem.* **15**, 283 (1975).
24. K. DENBIGH, "The Principles of Chemical Equilibrium," 2nd ed., p. 178, Cambridge Univ. Press, London/New York (1968).